

The next nearest neighbor effect on the 2D materials properties

Maher Ahmed

Department of Physics and Astronomy,

University of Western Ontario, London ON N6A 3K7, Canada and

Physics Department, Faculty of Science,

*Ain Shams University, Abbsai, Cairo, Egypt**

Abstract

In this work, the effect of introducing next nearest neighbor (NNN) hopping to the 2D materials was studied using the graphene 2D honeycomb two sublattice as an example. It is found that introducing NNN to the 2D materials removes the symmetry around the Fermi level and shifts it, at a small value of NNN hopping. This effect increases with increasing NNN hopping. If the NNN hopping becomes competitive with nearest neighbor (NN) hopping, the dispersion relations of the 2D materials changes completely from NN hopping dispersion relations. The results show that the 2D material sensitivity for NNN hopping effect is much larger in the 2D honeycomb lattice than 2D square lattice. This is due to the fact that the number of NNN sites is equal to six, which is the double of NN sites in the 2D honeycomb lattice. Meanwhile, the number of NNN sites is equal to four which is equal to NN sites in 2D square lattice. We therefore conclude that by changing the ratio between NNN and NN sites in the 2D lattice one can tune the sensitivity for NNN hopping effects.

* mahmed62@uwo.ca

I. INTRODUCTION

It is shown in [1–4] that the physical properties of 2D materials like graphene and magnetic stripes are mainly attributed to both their lattice structure and range of interactions between its sites. With fixing the range of interactions to include only the nearest neighbor hopping, a comparison between the obtained results of the 2D square lattice, zigzag edged, and armchair edged 2D honeycomb lattice show that the 2D lattice structure and its edge configuration play very important rule in its dispersion relations and consequently its possible applications.

Despite this importance of lattice structure in the properties of 2D materials, experiments and theories [5–8] show that increasing the range of the interaction to include the next nearest neighbor (NNN) in the graphene 2D honeycomb lattice changing its dispersion relations by removing dispersion symmetry around the Fermi level with shifting Fermi level value, and changing their behavior around the impurities in the lattice [9]. Also, including the next nearest neighbor hopping in 2D square lattice changing its dispersion relations [10].

It is interesting to study the effect of introducing the next nearest neighbor in the structure of the hopping \mathbf{E} matrix, and consequently on the obtained dispersion relations and the localized edge states of the 2D materials which has not been previously examined.

In this work, the graphene Hamiltonian [6] which includes the next nearest neighbor interaction term will be used to study its effect on the dispersion relations, edge states, and impurities states in the graphene nanoribbons with zigzag and armchair edge. The obtained results should also be applicable to the magnetic case, since the next nearest neighbor interaction term can be added to Heisenberg Hamiltonian [11, 12].

II. THEORETICAL MODEL

The system initially under study is a 2D graphene nanoribbon in the xy -plane. The crystallographic description of graphene honeycomb lattice is given in [6]. The nanoribbon is of finite width in the y direction with N atomic rows (labeled as $n = 1, \dots, N$) and it is infinite in x direction ($-\infty \Leftrightarrow \infty$). The total Hamiltonian of the system is given by

$$\hat{H} = - \sum_{\langle ij \rangle} t_{0ij} (\mathbf{a}_i^\dagger \mathbf{b}_j + \mathbf{h.c.}) + t_{1ij} (\mathbf{a}_i^\dagger \mathbf{a}_j + \mathbf{b}_i^\dagger \mathbf{b}_j + \mathbf{h.c.}), \quad (1)$$

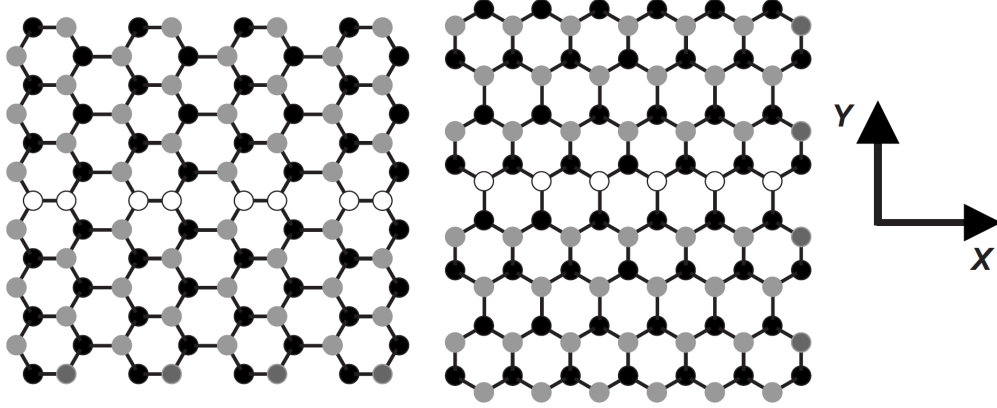


FIG. 1. Armchair (left) and zigzag (right) graphene 2D honeycomb nanoribbons in xy -plane, where black (gray) dots are the sublattice A(B) with a line of impurities (white dots) in the middle of the sheet, with average spin alignment in z direction. The stripes are finite in y direction with N rows ($n = 1, \dots, N$) and they are infinite in the x direction. Figure taken from [13].

where the first term $t_{0ij} (\approx 2.8\text{eV})$ is the nearest-neighbor hopping energy and in graphene it is the hopping between different sublattices A and B . Also $t_{1ij} (\approx 0.1\text{eV})$ is the next nearest-neighbor hopping energy which here in graphene is the hopping in the same sublattice [6–8]. The summations over i and j run over all the sites where i and j are belong to different sublattice A(B) for the nearest neighbors hopping term, and they are belonging to the same sublattice for the next nearest-neighbor hopping energy. Where the nearest neighbor hopping t_{0ij} has a constant “bulk” value t when either i and j are in the interior of the nanoribbon, and another constant value t_e when i and j are both at the edge of the nanoribbon (i.e., in row $n = 1$ or $n = N$). Similarly, for the next nearest-neighbor hopping energy t_{1ij} , we assume that it has a constant value t' when the site i is inside the nanoribbon, and it is equal to t'_e for sites at the edge of the nanoribbon.

Since the nanoribbon extends to $\pm\infty$ in the x direction, we may introduce a 1D Fourier transform to wavevector q_x along the x direction for the fermions operators a_i^\dagger (a_i) and b_j^\dagger (b_j) as follows:

$$\begin{aligned}
 b_j(x) &= \frac{1}{\sqrt{N_0}} \sum_n b_n(q_x) e^{-i\mathbf{q}_x \cdot \mathbf{r}_j} & b_j^\dagger(x) &= \frac{1}{\sqrt{N_0}} \sum_n b_n^\dagger(q_x) e^{i\mathbf{q}_x \cdot \mathbf{r}_j} \\
 a_i(x) &= \frac{1}{\sqrt{N_0}} \sum_n a_n(q_x) e^{-i\mathbf{q}_x \cdot \mathbf{r}_i} & a_i^\dagger(x) &= \frac{1}{\sqrt{N_0}} \sum_n a_n^\dagger(q_x) e^{i\mathbf{q}_x \cdot \mathbf{r}_i}.
 \end{aligned} \tag{2}$$

Here N_0 is the (macroscopically large) number of spin sites in any row, \mathbf{q}_x is a wavevector in the first Brillouin zone of the reciprocal lattice and both \mathbf{r}_i and \mathbf{r}_j is the position vectors of any carbon

sites i and j . The new operators obey the following commutation relations:

$$\left[a_n(q_x), a_n^\dagger(q'_x) \right] = \delta_{q_x q'_x}, \quad \left[b_n(q_x), b_n^\dagger(q'_x) \right] = \delta_{q_x q'_x}. \quad (3)$$

Also, we define the hopping sum:

$$\begin{aligned} \tau(q_x) &= \sum_{\nu} t_{0ij} e^{-i\mathbf{q}_x \cdot (\mathbf{r}_i - \mathbf{r}_j)}. \\ \tau'(q_x) &= \sum_{\nu'} t_{1ij} e^{-i\mathbf{q}_x \cdot (\mathbf{r}_i - \mathbf{r}_j)}. \end{aligned} \quad (4)$$

The sum for the hopping terms $t_{0/1ij}$ is taken to be over all ν nearest neighbors and over all ν' next nearest-neighbor in the lattice which depends on the edge configuration as zigzag or armchair for the stripe. For the armchair configuration, the hopping sum for nearest neighbors gives the following factors $\tau_{nn'}(q_x)$

$$\tau_{nn'}(q_x) = t \left[\exp(iq_x a) \delta_{n',n} + \exp\left(i\frac{1}{2}q_x a\right) \delta_{n',n\pm 1} \right] \quad (5)$$

and for the zigzag configuration, it gives

$$\tau_{nn'}(q_x) = t \left[2 \cos\left(\frac{\sqrt{3}}{2}q_x a\right) \delta_{n',n\pm 1} + \delta_{n',n\mp 1} \right]. \quad (6)$$

The hopping sum for next nearest neighbors gives the following factors $\tau'_{nn'}(q_x)$

$$\tau'_{nn'}(q_x) = t' \left[\delta_{n',n\pm 2} + 2 \cos(q_x a 3/2) \delta_{n',n\pm 1} \right] \quad (7)$$

for the armchair configuration, and

$$\tau_{nn'}(q_x) = 2t' \left[\cos(\sqrt{3}q_x a) \delta_{n',n} + \cos(\sqrt{3}q_x a/2) \delta_{n',n\pm 2} \right] \quad (8)$$

for the zigzag configuration case, where the \pm sign, in all the above factors, depends on the sublattice since the atom line alternates from A and B.

Substituting Equations (2) and (4) in Equation (1), and rewriting the summation over nearest and next nearest neighbors sites, we get the following form of the operator term \hat{H} :

$$\hat{H} = - \sum_{nn'} \tau'(q_x) \left(a_n^\dagger a_{n'} + b_n^\dagger b_{n'} \right) + \tau(q_x) a_n b_{n'}^\dagger + \tau(-q_x) a_n^\dagger b_{n'}. \quad (9)$$

The first terms count the elementary excitations on each sublattice, while the second describes the coupling between the sublattices.

In order to diagonalize \hat{H} and obtain the dispersion relations for graphene nanoribbons, we may consider the time evolution of the creation and the annihilation operators a_i^\dagger (a_i) and b_j^\dagger (b_j), as

calculated in the Heisenberg picture in quantum mechanics where the time dependent is transferred from the system wavefunction to the operators. In this case, the equations of motion (using the units with $\hbar = 1$) for the annihilation operators $a_i(b_j)$ are as follows [14–18]:

$$\begin{aligned}\frac{da_n}{dt} &= i[H, a_n] \\ &= i \sum_{nn'} -\tau'(q_x)a_{n'} - \tau(-q_x)b_{n'}\end{aligned}\quad (10)$$

and

$$\begin{aligned}\frac{db_n}{dt} &= i[H, b_n] \\ &= i \sum_{nn'} -\tau'(q_x)b_{n'} - \tau(q_x)a_{n'}\end{aligned}\quad (11)$$

where the commutation relation in Equation (3) was used, as well as the operator identity $[AB, C] = A[B, C] + [A, C]B$.

The electronic dispersion relations of the graphene (i.e., energy or frequency versus wavevector) can now be obtained by solving the above operator equations of motion. The electronic energy can be expressed in terms of the frequency using the relation $E = \hbar\omega$, and assuming that electronic energy modes behave like $\exp[-i\omega(q_x)t]$, on substituting this time dependent in Equations and , we get the following sets of coupled equations:

$$\omega(q_x)a_n = \sum_{nn'} \tau'_{nn'}(q_x)a_{n'} + \tau_{nn'}(-q_x)b_{n'}\quad (12)$$

$$\omega(q_x)b_n = \sum_{nn'} \tau_{nn'}(q_x)a_{n'} + \tau'_{nn'}(q_x)b_{n'}\quad (13)$$

The above equations can be written in matrix form as following

$$\omega(q_x) \begin{bmatrix} a_n \\ b_n \end{bmatrix} = \begin{bmatrix} T'(q_x) & T(q_x) \\ T^*(q_x) & T'(q_x) \end{bmatrix} \begin{bmatrix} a_n \\ b_n \end{bmatrix}\quad (14)$$

where the solution of this matrix equation is given by the condition

$$\det \begin{bmatrix} -(\omega(q_x)I_N - T'(q_x)) & T(q_x) \\ T^*(q_x) & -(\omega(q_x)I_N - T'(q_x)) \end{bmatrix} = 0\quad (15)$$

Where $T(q_x)$ and $T'(q_x)$ are nearest and next nearest exchange matrices respectively, which are depend on the orientation of the ribbon, and $\omega(q_x)$ are the energies of the modes. The matrix $T(q_x)$

TABLE I. Nearest neighbor hopping matrix elements for the graphene as 2D honeycomb lattice

Parameter	Zigzag	Armchair
α	0	$te^{-iq_x a}$
β	$2t \cos(\sqrt{3}q_x a/2)$	$te^{iq_x a/2}$
γ	t	$te^{iq_x a/2}$

TABLE II. Next nearest neighbor hopping matrix elements for the graphene as 2D honeycomb lattice

Parameter	Zigzag	Parameter	Armchair
ϵ	$2t' \cos(\sqrt{3}q_x a)$	θ	t'
ζ	$2t' \cos(\sqrt{3}q_x a/2)$	η	$2t' \cos(q_x a/2)$

is given by

$$\begin{pmatrix} \alpha & \beta & 0 & 0 & \cdots \\ \beta & \alpha & \gamma & 0 & \cdots \\ 0 & \gamma & \alpha & \beta & \cdots \\ 0 & 0 & \beta & \alpha & \cdots \\ \vdots & \vdots & \vdots & \vdots & \ddots \end{pmatrix}. \quad (16)$$

The matrix $T'(q_x)$ for zigzag ribbon is given by

$$\begin{pmatrix} \epsilon & 0 & \zeta & 0 & 0 & \cdots \\ 0 & \epsilon & 0 & \zeta & 0 & \cdots \\ \zeta & 0 & \epsilon & 0 & \zeta & \cdots \\ 0 & \zeta & 0 & \epsilon & 0 & \cdots \\ 0 & 0 & \zeta & 0 & \epsilon & \cdots \\ \vdots & \vdots & \vdots & \vdots & \vdots & \ddots \end{pmatrix} \quad (17)$$

and the matrix $T'(q_x)$ for armchair ribbon is given by

$$\begin{pmatrix} 0 & \eta & \theta & 0 & 0 & \cdots \\ \eta & 0 & \eta & \theta & 0 & \cdots \\ \theta & \eta & 0 & \eta & \theta & \cdots \\ 0 & \theta & \eta & 0 & \eta & \cdots \\ 0 & 0 & \theta & \eta & 0 & \cdots \\ \vdots & \vdots & \vdots & \vdots & \vdots & \ddots \end{pmatrix} \quad (18)$$

The parameters $\alpha, \beta, \gamma, \epsilon, \zeta, \theta$ and η depend on the stripe edge geometry and are given in Tables I and II.

A. Neglecting the next nearest neighbor hopping as special case

The next nearest neighbor hopping t' can be neglected compared to nearest neighbor hopping t , in this case the $T'(q_x)$ is equal to zero matrix $\mathbf{0}$ and Equation (14) become as following

$$\det \begin{bmatrix} -(\omega(q_x)I_N) & T(q_x) \\ T^*(q_x) & -(\omega(q_x)I_N) \end{bmatrix} = 0 \quad (19)$$

which is the result obtained before for graphene ribbons using the tight binding model with neglecting NNN hopping [13]. It is also very similar to the case of magnetic stripes in [2], which do not have NNN exchange, the only difference between the magnetic case and TBM graphene without NNN hopping is the effect of α , i.e. insite energy.

III. NUMERICAL CALCULATIONS

The dispersion relations for the above graphene nanoribbons are obtained numerically as the eigenvalues [19, 20] for the matrix Equation (14). This is very similar to graphene with only (NN) [2], and therefore the same numerical calculations method used there will be used here to get its solutions.

IV. RESULTS

To compare our results for NN and NNN interaction with the tight-binding Hamiltonian, with only NN interactions, we choose our stripes sizes, scaling our result to be dimensional less quantities, and choose physical parameters matched that ones used in reference [13] for graphene.

Figures 2 shows the effect of next nearest neighbor interaction in the dispersion relations, edge states, and impurities states in the graphene zigzag nanoribbons, as expected all Figure show the removing dispersion symmetry around the Fermi level with shifting the Fermi level value toward valance band. Figure 2 (a) and (b) show the effect for the next nearest neighbor value of $t' = 0.036t$, which correspond to $t' \approx 0.1$ eV and $t \approx 2.8$ eV given in references [6, 7], The changing in the dispersion symmetry around the Fermi level with shifting the Fermi level value toward valance

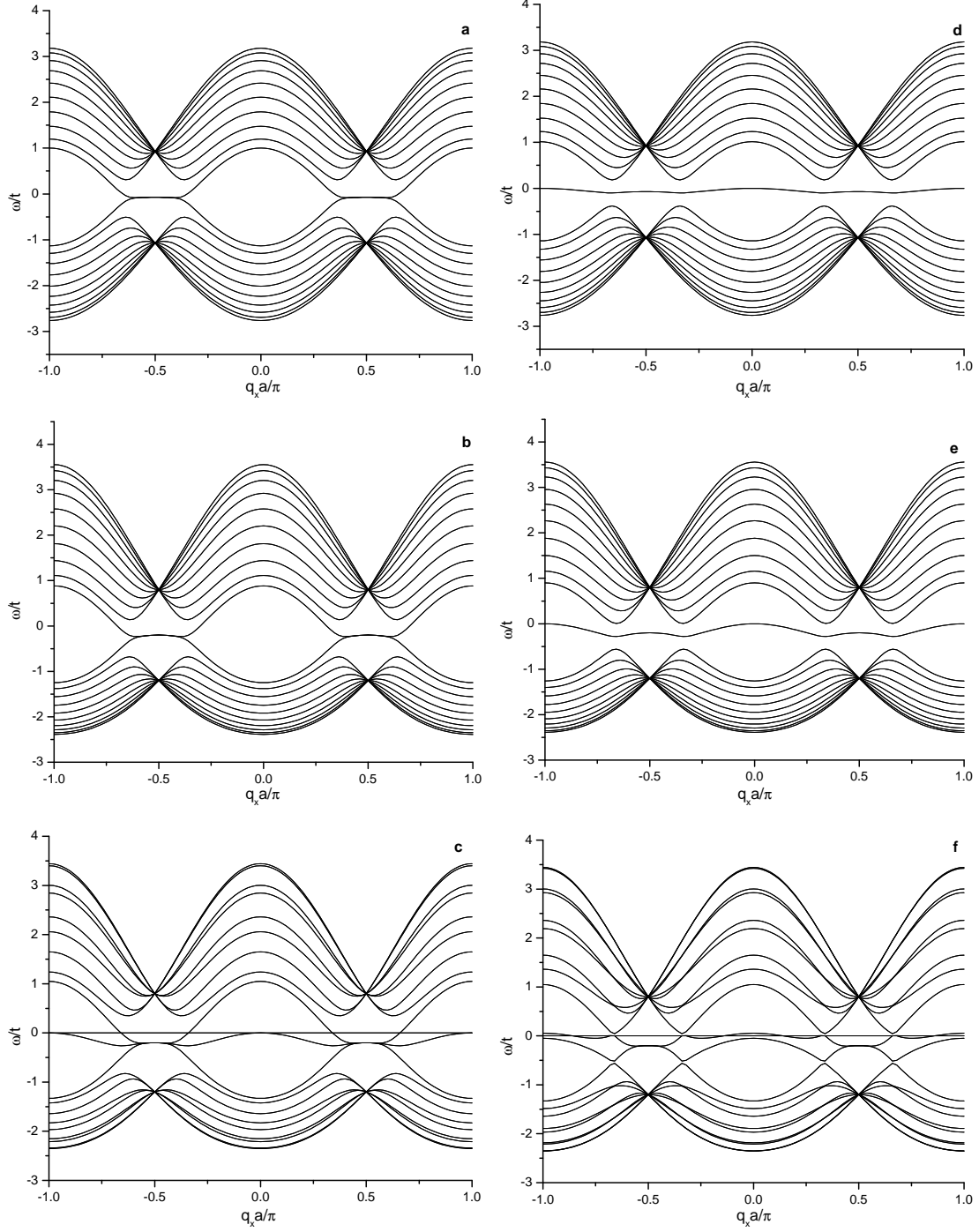


FIG. 2. The effect of next nearest neighbor interaction in the dispersion relations, edge states, and impurities states in the graphene zigzag nanoribbons. Right side stripe width $N = 20$ (a) $t' = 0.036t$ (b) $t' = 0.1t$ (c) $t' = 0.1t$ and with impurities line at row number 11 with $J_I = 0$. Left side stripe width $N = 21$ (d) $t' = 0.036t$ (e) $t' = 0.1t$ (f) $t' = 0.1t$ and with impurities line at row number 11 with $J_I = 0$.

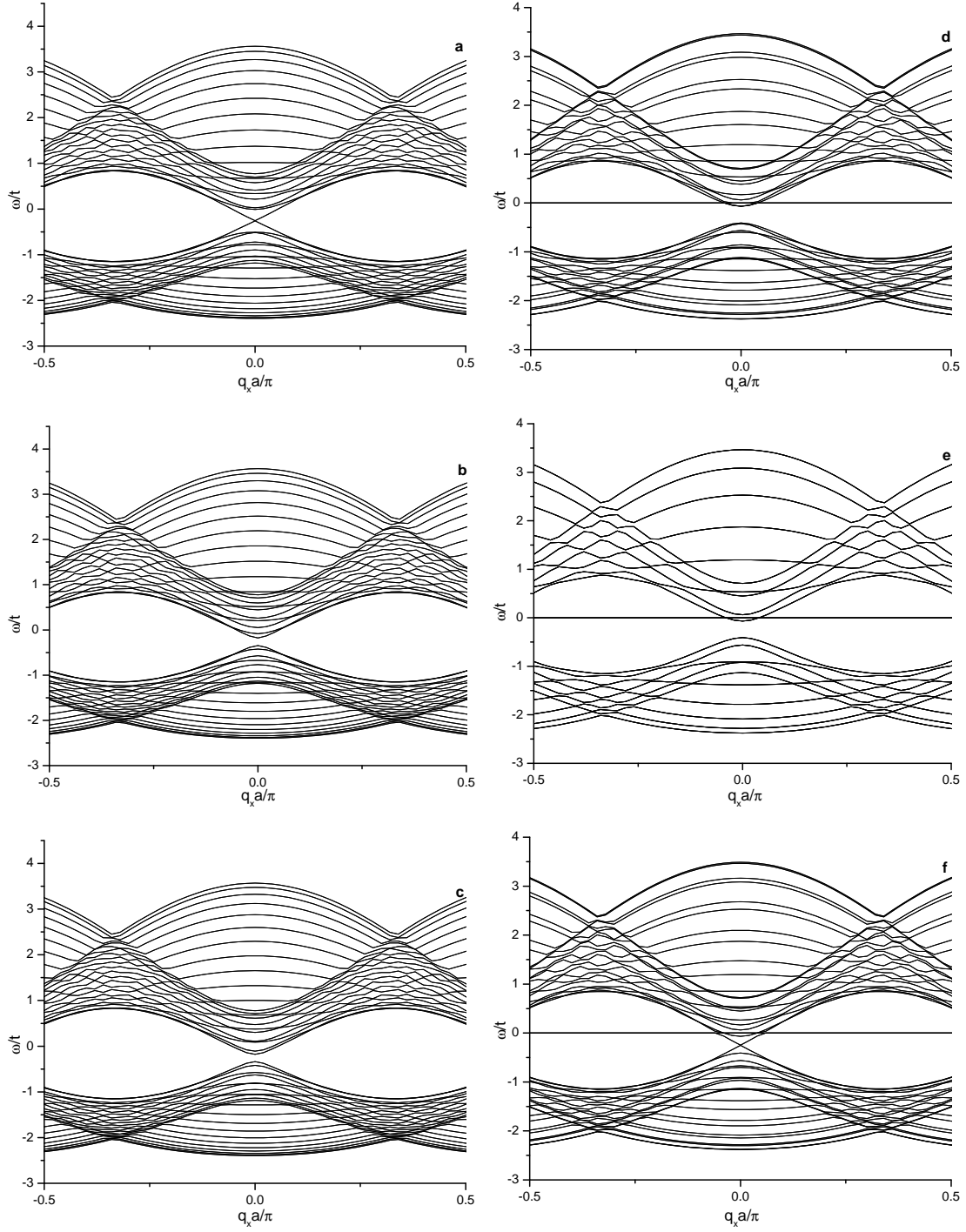


FIG. 3. The effect of next nearest neighbor interaction in the dispersion relations, band gap, and impurities states in the graphene armchair nanoribbons. Right side $t' = 0.1t$ for stripe width (a) $N = 20$ (b) $N = 21$ (c) $N = 22$. Left side $t' = 0.1t$ and with impurities line at row number 11 with $J_I = 0$ for stripe width (a) $N = 20$ (b) $N = 21$ (c) $N = 22$.

band is small compared by the obtained results in [2] for the same zigzag nanoribbons without NNN interaction, as the value of NNN increases to $t' = 0.1t$ as shown in Figure 2 (c) and (d) the density of states increase in the conduction band (high energy levels) and decreasing in the valance band (low energy levels) removing the symmetry around the Fermi level and shifting it. The Figures show that including NNN effecting the flatness of the edge localized states of zigzag graphene nanoribbons but not effecting its position in Fermi Level, as the NNN increase the flatness decreases which reflect the introducing of q_x depends for hopping in edge sites, which more clear for the extended localized edge state in zigzag with width $N = 21$.

Figures 2 (e) and (f) show the effect of NNN on the impurities states in the zigzag nanoribbons. It is clear that the position of energy state of impurities line not affected by including NNN, which is a result of not participating for the impurities in NNN hopping in this calculation. But introducing the NNN hopping in the lattice shifting the Fermi level and changing the density of the states around the impurities level. As, NNN increase the impurities level move to more density of states region, this explain the appearance of impurities level as a moving peak in the density of states for the graphene, with increasing surrounding density of states as NNN increasing [10].

Figures 3 show the effect of next nearest neighbor interaction in the dispersion relations, and impurities states in the graphene armchair nanoribbons. The behavior in the armchair case with including NNN is very similar to the zigzag case given above for removing the symmetry around the Fermi level, shifting it, and its effect in the impurities level relative position to Fermi level. There is no any effect on the absence of edge states in armchair nanoribbons and on their band shape at $q_x a/\pi = 0$ with including NNN in the model.

V. DISCUSSION AND CONCLUSIONS

In this work, the effect of introducing NNN hopping to the 2D materials was studied using the graphene 2D honeycomb two sublattice as example. Including the NNN in the model add NNN hopping matrix $T'(q_x)$, which depending on the momentum q_x in the direction of nanoribbons symmetry, to the diagonal sub matrices αI_N in the \mathbf{E} matrix. This shows that NNN hopping matrix $T'(q_x)$ is real and is describing the hopping with translation motion in the sublattice sites in both zigzag and armchair stripes.

When t' is equal to very small percentage of t , the probability is very small for the particles to hopping in the same sublattice by NNN hopping and consequently the net number of particles

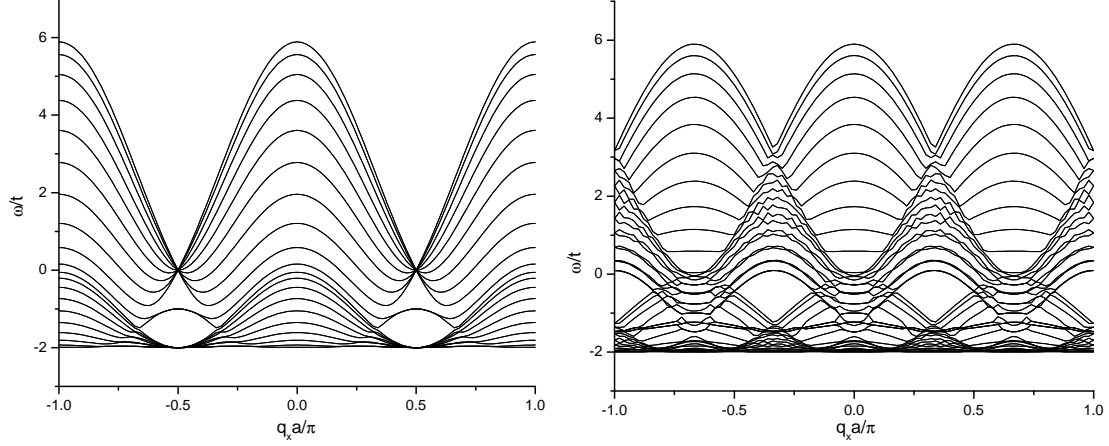


FIG. 4. The effect of high next nearest neighbor interaction $t' = 0.5t$ in the dispersion relations on zigzag left side and armchair right side lattice with width $N = 20$.

in NNN hopping is very small which result a small effect in the dispersion relations of only NN hopping. As the percentage increases, the probability for NNN hopping increases, and consequently the net number of particles in NNN hopping increases. This results in an increasing effect in the dispersion relations of only NN hopping. The main effect of NNN hopping in small range is changing the density of states for dominated NN hopping dispersion relations, which can be explained as following: since the probability for the particles to hopping in the same sublattice by NNN hopping is increasing with increasing its energy and consequently the net number of particles from every mode that able to do NNN hopping is proportional to the mode energy. The highest energy mode has the highest percentage number of particles that participating in NNN hopping, this percentage of particles decreases with decreasing the energy of the mode, most of this NNN particles will be trapped in low energy modes. The overall effect is the available particles densities is lowest in high energy modes and highest in low energy modes. This means that the available momentum spaces in high energy modes is increased for particles in NN hopping due to NNN effect consequently the density of states is increased in high energy modes, while the available momentum spaces in low energy modes is decreased for particles in NN hopping due to NNN effect consequently the density of states is decreased in low energy modes. This removing the symmetry around the Fermi level and shifting it, this effect increases with increasing NNN hopping. If the NNN hopping become competitive with NN hopping the dispersion will changing completely as seen in Figure 4.

The above results for NNN hopping is applied to 2D square lattices as shown in Figure 5 by

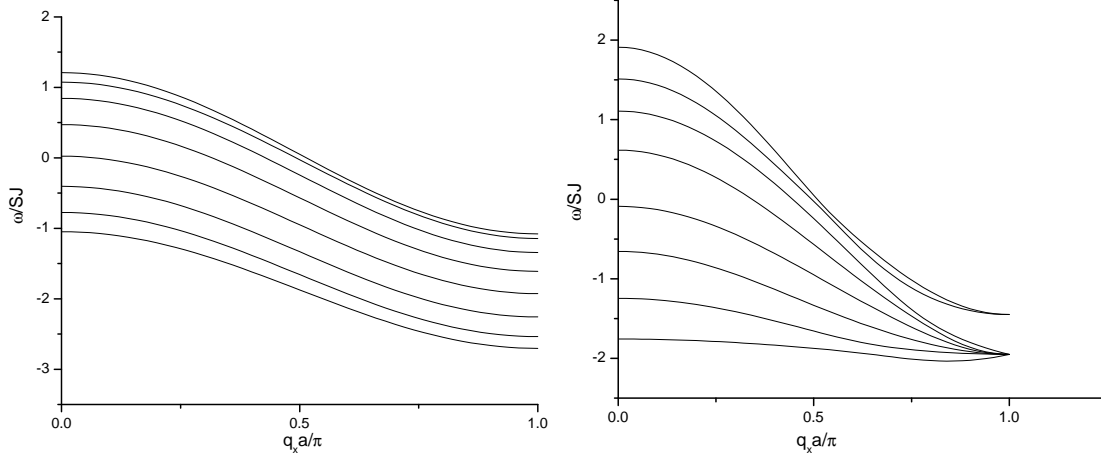


FIG. 5. The effect of next nearest neighbor interaction in the dispersion relations on magnetic 2D square lattice with width $N = 8$. Right side $t' = 0.1t$ left side $t' = 0.5t$.

adding the term $(SJ'/2)(2 \cos(q_x a))$ in upper and lower off diagonal of its \mathbf{E} matrix. The result show the same behavior for the density of states.

The comparison between the results of $t' = 0.1t$ between 2D honeycomb lattice and 2D square lattice show that the sensitivity for NNN hopping effect is much larger in the 2D honeycomb lattice than 2D square lattice, this due to the fact that the number of NNN sites is equal to six which is the double of NN sites in the 2D honeycomb lattice, while the number of NNN sites is equal to four which is equal to NN sites in 2D square lattice. Therefore by changing the ratio between NNN and NN sites in the 2D lattice one can tune the sensitivity for NNN hopping effects.

ACKNOWLEDGMENTS

This research has been supported by the Egyptian Ministry of Higher Education and Scientific Research (MZA).

-
- [1] M. Z. Ahmed, *Study of electronic and magnetic excitations in the 2D materials represented by graphene and magnetic nano-ribbons*, Ph.D. thesis, The University of Western Ontario (2011), download pdf version and a Viedo on Sciencestage.com.
- [2] M. Ahmed, (2011), arXiv:1110.5716v1 [cond-mat.mes-hall].

- [3] M. Ahmed, (2011), arXiv:1110.5105v1 [cond-mat.mes-hall].
- [4] M. Ahmed, (2011), arXiv:1110.6488v1 [cond-mat.mes-hall].
- [5] J. Barrios-Vargas and G. G. Naumis, (Mar 2011), arXiv:1103.0960v1 [cond-mat.mtrl-sci].
- [6] A. H. Castro Neto, F. Guinea, N. M. R. Peres, K. S. Novoselov, and A. K. Geim, *Rev. Mod. Phys.* **81**, 109 (2009).
- [7] R. S. Deacon, K.-C. Chuang, R. J. Nicholas, K. S. Novoselov, and A. K. Geim, *Phys. Rev. B* **76**, 081406 (2007).
- [8] S. Reich, J. Maultzsch, C. Thomsen, and P. Ordejón, *Phys. Rev. B* **66**, 035412 (2002).
- [9] Y. V. Skrypnik and V. M. Loktev, *Phys. Rev. B* **73**, 241402 (2006).
- [10] K. Sun, Z. Gu, H. Katsura, and S. Das Sarma, *Phys. Rev. Lett.* **106**, 236803 (2011).
- [11] D. S. Xue, M. Z. Gao, J. B. Yang, Y. Kong, and F. S. Li, *physica status solidi (b)* **193**, 161 (1996).
- [12] M. S. Seehra and T. M. Giebultowicz, *Phys. Rev. B* **38**, 11898 (1988).
- [13] R. N. Costa Filho, G. A. Farias, and F. M. Peeters, *Phys. Rev. B* **76**, 193409 (2007).
- [14] D. R. Bs, *Quantum mechanics: a modern and concise introductory course* (Springer, 2007).
- [15] R. L. Liboff, *Introductory Quantum Mechanics*, 1st ed. (Longman Higher Education, 1987).
- [16] L. Kantorovich, *Quantum Theory of the Solid State: An Introduction* (Springer, 2004).
- [17] U. Ressler, *Solid State Theory: An Introduction* (Springer, 2009).
- [18] K. F. Henrik Bruus, *Many-body quantum theory in condensed matter physics: an introduction* (Oxford University Press, 2004).
- [19] J. R. M. Karim M. Abadir, *Matrix algebra*, Vol. 1 (Cambridge University Press, 2005).
- [20] W. H. Press, *Numerical recipes in FORTRAN :the art of scientific computing*, Vol. 1 (Cambridge University Press, Cambridge England ; New York, 1992) p. 963.